Elkassas *et al.*
Journal of Engineering and Applied Science (2022) 69:86
https://doi.org/10.1186/s44147-022-00123-2

Journal of Engineering and Applied Science

RESEARCH Open Access

Flexure behavior of hollow steel beams strengthening with ferrocement

Ehab Elkassas, Alaa M. Morsy and Mohamed Marzouck*

*Correspondence: mohamedmarzouck28@gmail.com

Construction and Building Engineering Department, Arab Academy for Science Technology and Maritime Transport, Cairo, Egypt

Abstract

Experimental and numerical studies are carried out to investigate the flexural behavior of precast lightweight composite beams composed of a hollow steel beam strengthened with a ferrocement layer. This composite beam comprises of a slender cold-formed hollow section of dimension (140 × 180 mm) of different thicknesses surrounded by a ferrocement layer. This composite beam is named a precast ferrocement cold-formed hollow section (FCH). Nine beams with a span of 1500 mm were tested under a four-point bending system to evaluate their flexural strength. Four different parameters have been examined, which are the spacing of shear connectors, ferrocement thickness, hollow steel section thickness, and the effect of surface friction. The test results showed that the presence of 30 mm ferrocement layer increased the capacity by 18% compared with the control specimen. The presence of shear connectors increases the capacity by 30%. Increasing the steel cross-section thicknesses increase section capacity by 16–33% and finally, increasing the surface friction has a very small effect on the section capacity, which can be neglected. The finite element models were developed and validated by the test results; results show a close agreement between the experimental and finite element results. Extensive parameters were investigated, which were mortar compressive strength (f'_c) and the position of the shear connectors. The results indicated that increasing mortar strength increases section capacity ranging between 11% and 18%. The presence of a shear connector in the web and the lower flange of the hollow section have an insignificant effect.

Keywords: Cold formed steel, Ferrocement, Composite beam, Local buckling, Shear connector

Introduction

In recent years, composite steel-concrete structural systems have become a popular design and construction technique. In comparison to traditional reinforced concrete beams, composite steel-concrete beams have numerous advantages, including lighter steel weight, longer span, and faster erection.

As the world's steel industry transitions from hot-rolled sections and plates to coil and strip, cold-formed steel (CFS) products are becoming more commonly employed in structural design. There are many shapes of cold-formed. This study focused on cold-formed hollow steel sections. Cold-formed hollow sections are now permitted in all

major structure design standards such as AISC 360-16 [1], BS 5950 [2], AS 4100 [3], and EC3 2004 [4].

The use of a thin plate in the hollow section can lead to flexural and local buckling failure, as described by Jouaux [5]. Design codes classify hollow steel sections into compact, non-compact, and slender sections based on their bending behavior. Design codes define compact sections as those that can reach plastic moments without local buckling, non-compact sections as those that can reach yield moments without local buckling, and slender sections as those that cannot reach yield moments due to local buckling. AISC 360-16 [1] gives a slender limit for classifying hollow sections. The flange is considered compact when the slender ratio (b/t) is less than $\left(1.12\sqrt{E/f_y}\right)$ and non-compact when it is less than $\left(1.40\sqrt{E/f_y}\right)$. The web is considered compact when the slender ratio (h/t) is less than $(2.42\sqrt{E/f_y})$ and non-compact when it is less than $(5.70\sqrt{E/f_y})$. This study focused on the slender sections, with flange slender limits ranging from 43 to 67 calculated according to AISC 360-16 [1].

Ferrocement is a Ferro (iron) and cement mortar composite. Ferrocement is a type of thin-walled reinforced concrete in which wire mesh layers are distributed uniformly throughout the matrix. The ACI 549 committee [6] explained that ferrocement is a type of reinforced concrete that behaves differently than conventional reinforced concrete in which the reinforced elements are dispersed throughout the matrix. According to the ACI Committee, the ferrocement matrix consists of fine sand passed through sieve ASTM No. 8 (2.36 mm), with a sand–cement ratio by weight ranging from 1.5 to 2.5 and a water-cement ratio ranging from 0.35 to 0.5. Naaman [7] outlined the mechanical properties of ferrocement. According to Naaman, ferrocement has homogenous isotropic properties in two directions, high tensile strength that is of the same order as its compressive strength, high reinforcement ratio, and good durability under environmental exposures.

Many researchers have studied the behavior of composite sections composed of concrete and cold-formed steel under bending and compression. Alhajri [8] et al. outlined experimental and numerical studies to examine the structural behavior of nine precast U-shaped composite beams. These composite beams are comprised of a lipped channel section back-to-back and a 50 mm ferrocement slab. The study investigated the effect of the number of wire mesh and thickness of steel sections on structural behavior. It was found that increases in the number of wire mesh as well as the steel thickness-increased section capacity.

Cheng-Tzu Thomas Hsu [9] et al. studied an experimental study of six new composite beams to investigate their structural behavior. The composite beam in this test was comprised of a reinforced concrete slab on a corrugated cold-formed metal deck, back to back cold-formed steel joists, and a continuous cold-formed furring shear connector. The study investigated the maximum moment capacity and deflection of specimens. It was found that a composite beam can reach its ultimate capacity without buckling due to this type of shear connector.

El-Sayed [10] et al. presented an experimental study to investigate the structural behavior of a cold-formed square hollow column section strengthened by mortar under compression. Three short columns and ten long columns are tested where local and global buckling is measured. The study examined the effect of the thickness of polymer

mortar on the capacity of the column. The results obtained showed that strengthening a column with mortar increases axial capacity.

In this study, a new type of precast lightweight composite beam was comprised of a slender cold-formed hollow section (CFS) strengthened by a ferrocement layer called a precast ferrocement cold-formed hollow steel section (FCH). This system could provide an alternative composite system for floor and roof in medium and small size buildings. The main problem of slender hollow sections is the local buckling before reaching yield. The objective of this study is to investigate the flexural behavior of a precast composite beam by performing experimental tests and finite element analysis. Different parameters were studied, which were spacing of shear connector, mortar thickness, hollow section thickness, increasing friction by using the diamond plate, mortar compressive strength (f'_c), and the position of the shear connectors.

Methodology

Experimental program

Nine simply supported beams were tested. The tests aimed to study the flexural behavior and the strength of a ferrocement encased cold-formed hollow steel beam with different parameters: mortar thickness, hollow steel thickness, and spacing of the shear connector. A four-point bending system is used in these tests.

Test specimens

All specimens were 1800 mm long and spanned 1500 mm between supports. Figure 1 shows the specimen's details. Four parameters are studied in these tests. The first parameter is the spacing of the shear connectors, which are (100, 200, and 300 mm), where bolts of diameter 6 mm and length of 25 mm are used as shear connectors with grade (8.8) as shown in Fig. 2. The second parameter is ferrocement thickness, which are 30 mm and 50 mm. The third parameter is cold-formed steel thickness, where 2, 2.5, and 3 mm are studied. The fourth parameter is the effect of surface friction where diamond plates are used to be compared with ordinary smooth plates. Figure 3 shows the diamond plate shape. All specimens are reinforced with one layer of welded wire mesh of a diameter of 1.5 mm. Table 1 summarizes the specimen's details.

All specimens were cast using the same batch of mortar to ensure that its properties were identical for all beams.

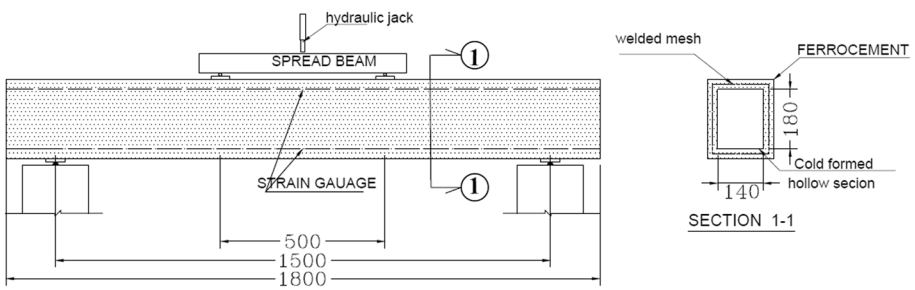

Fig. 1 Specimen details

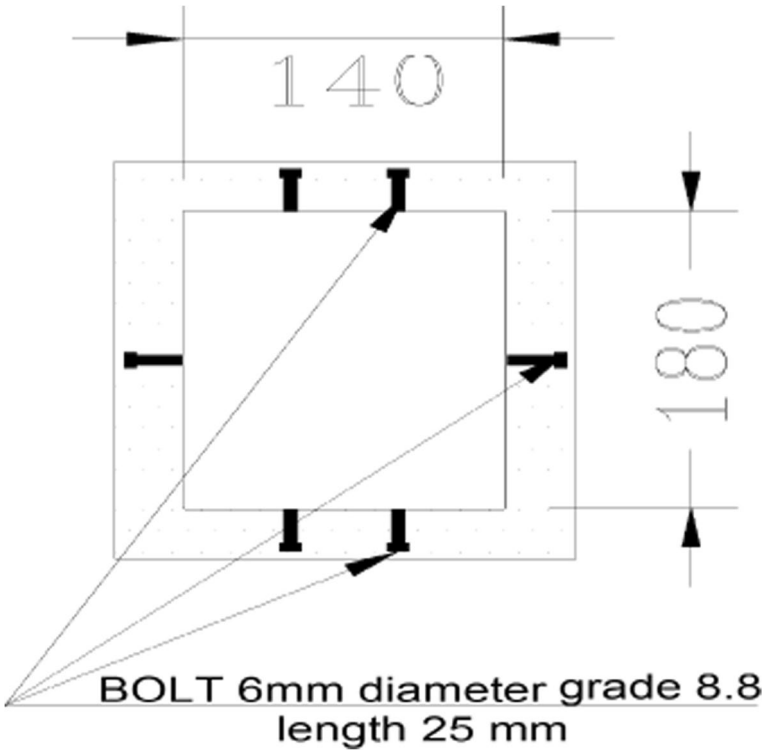

Fig. 2 Shear connector's positions

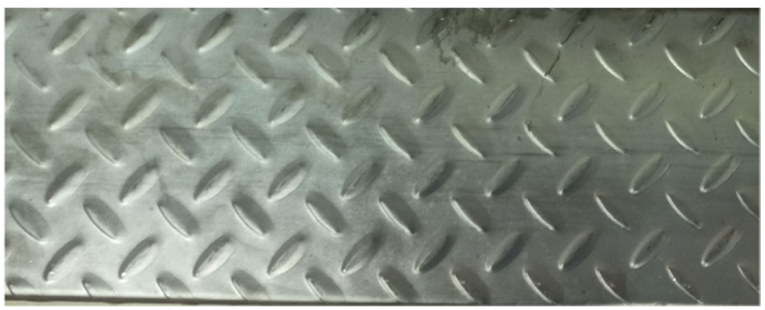

Fig. 3 Diamond plate shape

Test set up

A 400 KN capacity universal testing machine was used for the tests. A four-point bending system was applied. This system of loads produced a region of pure bending between point loads. Hence, the strength of the composite beam can be determined. The two-point loads were applied at a distance of 500 mm from the support. The spreader beam was applied to the specimen, and then the jack load from the jack was applied on it. Figure 4 shows the loads and instrumentation set-up. Test specimens were supported with roller and pinned supports so that they were simply supported beams. The deflections of specimens were recorded by dial gauge at mid-span. Strain gauges were installed at the top and bottom of hollow steel sections at mid-span to evaluate the stress-strain curves. Load increments of about 2 kN are used so

Table 1 Specimen's details

Specimens name	Mortar thickness (mm)	Steel thickness (mm)	Shear connector Spacing (mm)
CONTROL	–	2.5	–
FCH1	30	2.5	100
FCH2	30	2.5	200
FCH3	30	2.5	300
FCH4	30	2.5	N/A
FCH5	50	2.5	N/A
FCH6	50	2	N/A
FCH7	50	3	N/A
FCH8	50	2-(Diamond sheet)	N/A

N/A denote to without shear connector

Fig. 4 Load and instrumentation set up

that gradual failure of the specimen can be observed. The beams were loaded until failure. Rectangular steel plates of 7 cm width were used to distribute the load and prevent the premature failure due to concentrated load.

Properties of materials

Cold formed hollow section Three thicknesses (2, 2.5, and 3 mm) of the cold-formed hollow section were used in the tests. Figure 5 shows section dimensions. All cold-formed hollow steel sections in this study are un-galvanized. The grade of hollow sections is (St. 37) as indicated by manufactured.

Mortar The mortar matrix is comprised of ordinary Portland cement complying with ESS 373 [11] and ECC 203 [12] and sand passing through ASTM No. 8 (2.36 mm), free from any deleterious material. The mix proportion of sand/cement was 2/1 by weight, with a water-cement ratio of 0.5.

Six-cylinder specimens of size (75 × 150 mm) were also cast at the same time of casting to evaluate the compressive strength of mortar according to ACI 549 [6]. Cylinder compressive strength (f 'c) at day 28 is 23 N/mm^2.

Wire mesh Welded galvanized wire meshes are used in this study. The wire mesh surrounds the hollow steel beam in the middle of the ferrocement layer. The diameter

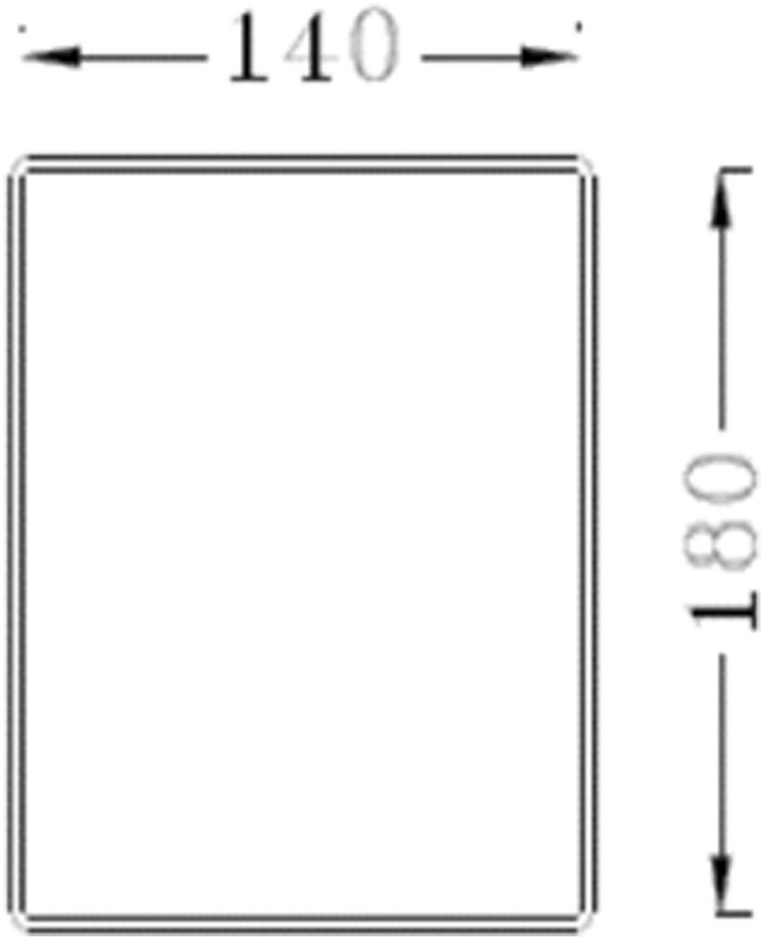

Fig. 5 Cold formed hollow section

Fig. 6 Welded wire mesh

of the wire mesh was 1.5 mm and the square opening diameter was (20 × 20 mm). Figure 6 shows the wire mesh shape. The grade of wire mesh is (St. 37) as indicated by manufactured.

Numerical study procedure

For numerical study, finite element models have been developed to investigate the behavior of precast composite beams. Ansys Mechanical APDL V19 software is used to create the F.E models. Figure 7 shows the finite element model. The models are built through the following steps: (a) geometric model using suitable elements, (b) material assignment, and (c) load and boundary conditions.

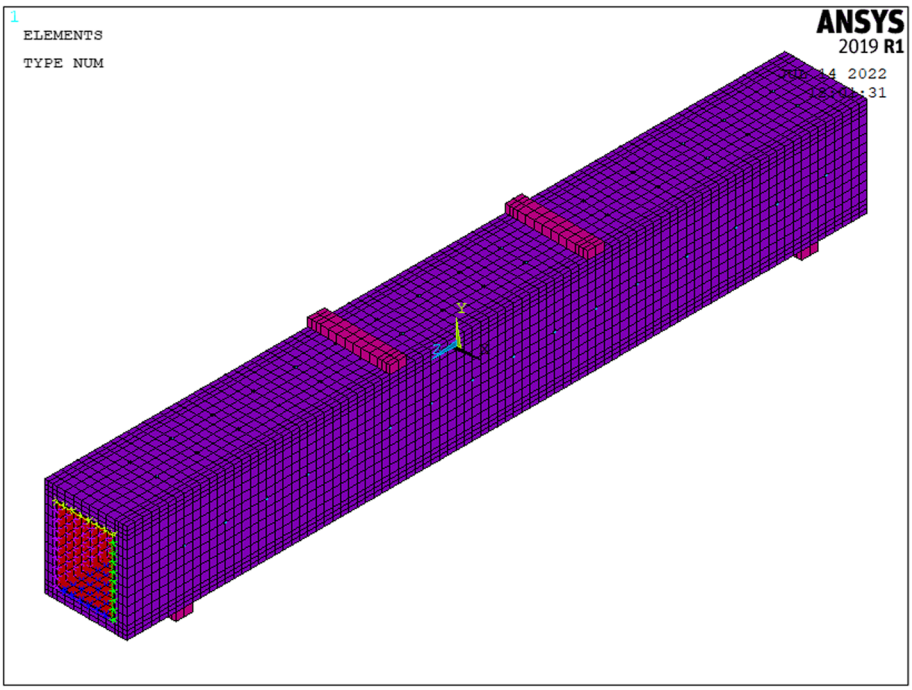

Fig. 7 Specimen's details

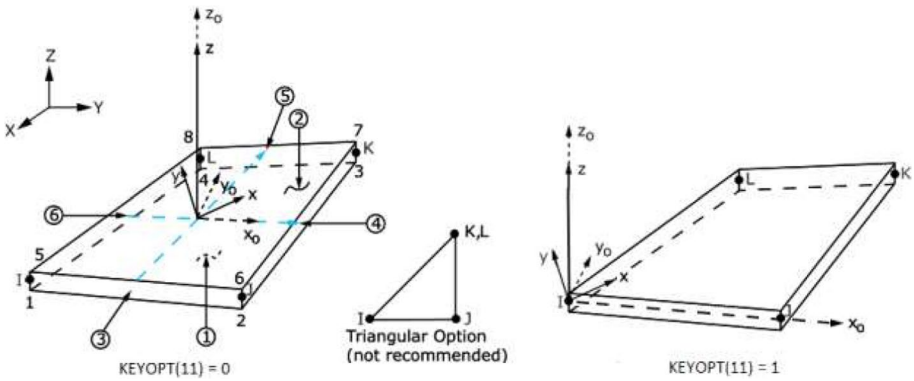

Fig. 8 SHELL 181 geometry, ANSYS

Geometric model

The accuracy of finite element models depends on the selection of suitable elements to predict the real behavior of members. These elements are mainly classified based on the features embedded in the element type. In this study, four different types of elements are used.

Cold formed box section The cold-formed section is modeled using a shell element (SHELL181). This element is used for the simulation of the thin wall structure. This element is defined as a four-node shell element where each node has 6 degrees of freedom (three *x*, *y*, and *z* in transition and three in rotation). Figure 8 shows element geometry.

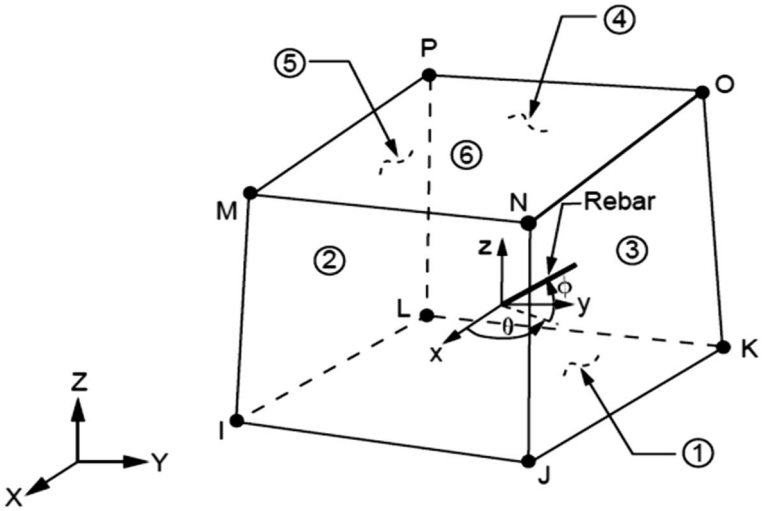

Fig. 9 Solid65 geometry, ANSYS

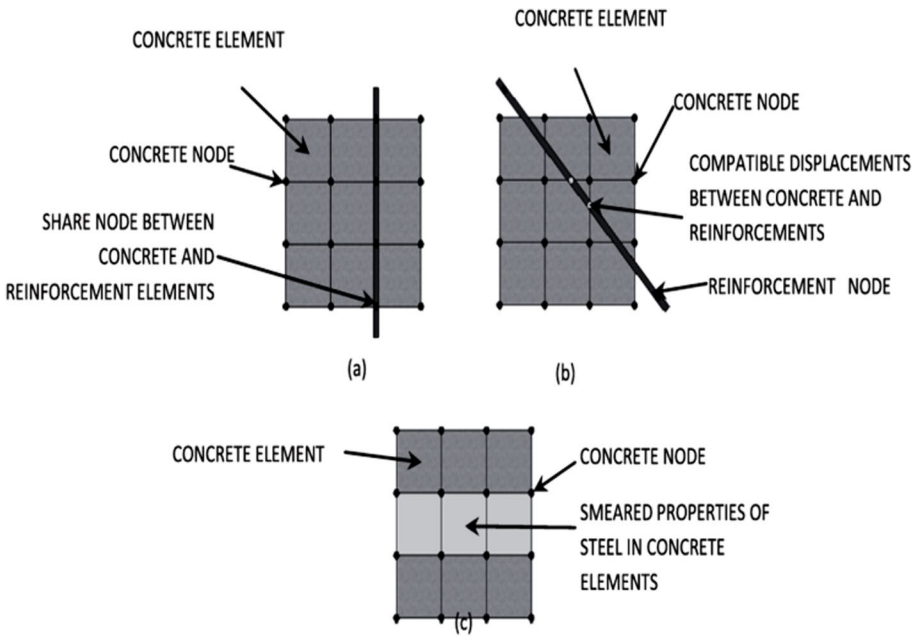

Fig. 10 Reinforced modeling techniques. **a** Discrete model. **b** Embedded model. **c** Smeared mode

Ferrocement layer Ferrocement is modeled using the Solid65 element. This element has eight nodes with 3 degrees of freedom at each node translation in the nodal *x*, *y*, and *z* directions. The element is capable of plastic deformation, cracking in three orthogonal directions, and crushing. Figure 9 shows element geometry. This element can simulate cracking under tension in three orthogonal directions, crushing under compression, plastic deformation, and creep. The following three techniques, which are shown in Fig. 10 are used to model steel reinforcement as described by Azimi et al. [13], which are (a) discrete model, (b) embedded model, and (c) smeared model. In this study, wire mesh

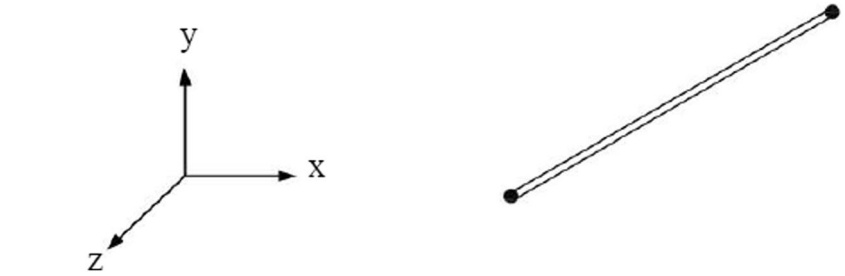

Fig. 11 Link 180 geometry, ANSYS

Fig. 12 Combin39 geometry, ANSYS

is modeled by a smeared model. The steel wire meshes were defined by the volume fraction, orientation angle, and initial strain.

Shear connector Link 180 is a uniaxial tension and compression element, and it is a 3D spar with 3 degrees of freedom at each node. The element is used to model 6 mm bolts, which are used as shear connectors. Figure 11 shows the geometry of link 180 element.

Interface modeling The first interface element, which is used to model friction between steel and concrete, is called the (contact-pair) element. The second interface element is (COMBIN39). This element can simulate the normal and dowel stiffness of shear connectors. This element is a unidirectional spring element with a nonlinear generalized force-deflection capability. The geometry of the COMBIN39 element is shown in Fig. 12. The load-slip relationship value for nonlinear spring element COMBIN39 is determined according to the following equation, which is presented by (Lorene and Kubica) [14]. This equation is used to determine the load-slip relationship for normal strength concrete.

$$\frac{P}{Pu} = \left(1 - e^{-0.55S}\right)^{0.3} \tag{1}$$

(Pu) is stud shear capacity, which is determined by ANSI/AISC 360-05 [1].

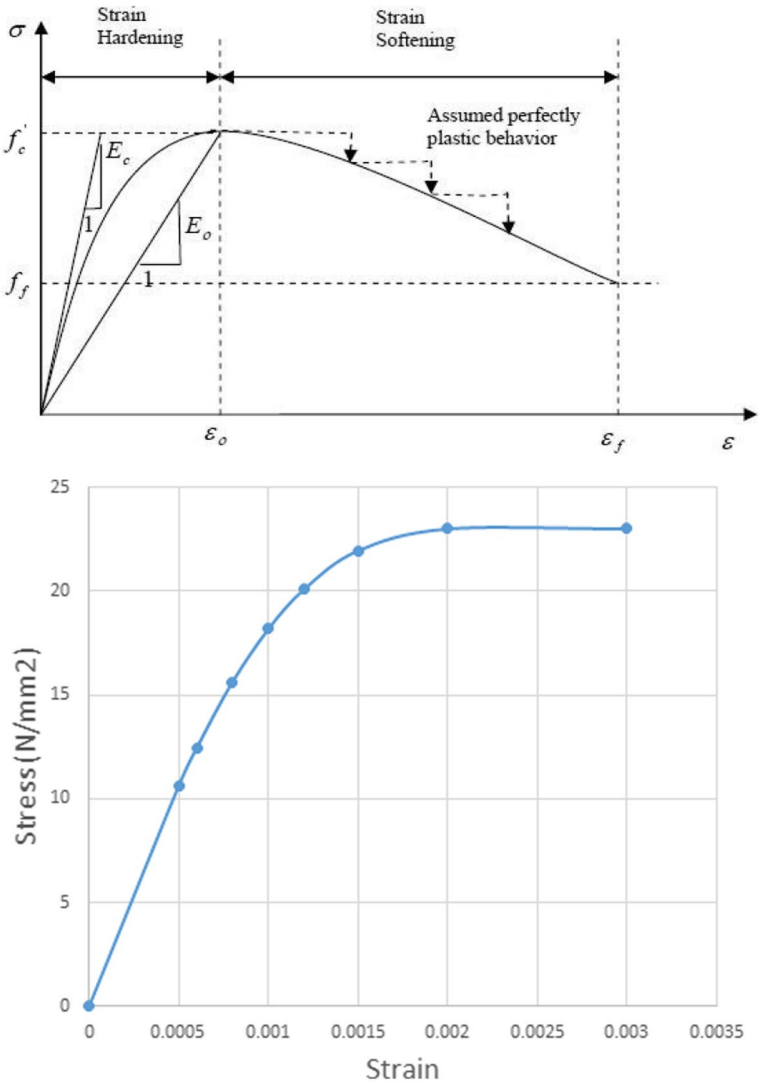

Fig. 13 Stress-strain curve under compression

Material

Mortar The nonlinear properties of mortar under compression, as shown in Fig. 13, are assigned to develop F.E models throughout the defining of stress-strain relations, which are developed by Desayi and Krishnan [15] through the following equations.

$$\mathrm{Fc} = \frac{\varepsilon.\mathrm{Ec}}{1 + \left(\frac{\varepsilon}{\varepsilon_0}\right)^2} \tag{2}$$

$$\varepsilon_0 = \frac{2\mathrm{Fc}}{\mathrm{Ec}} \tag{3}$$

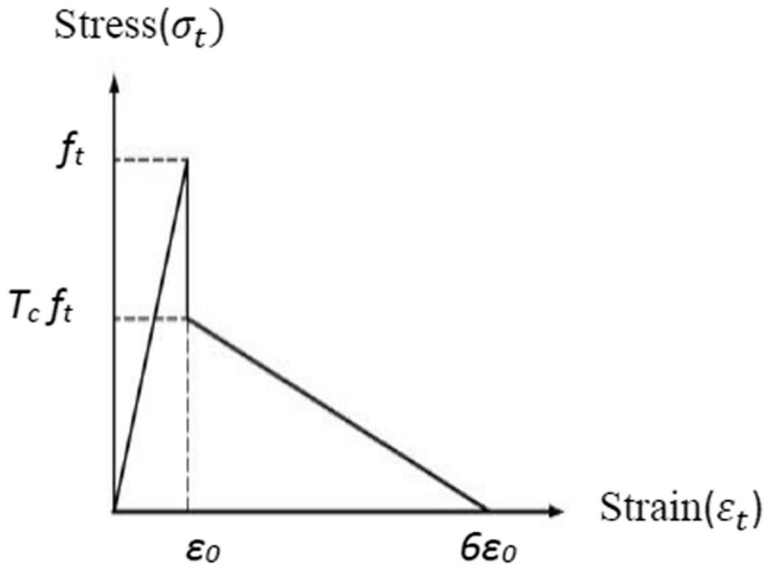

Fig. 14 Stress-strain curve under tension

Table 2 Experimental results

Specimens ID	Failure load (Pu) kN EXP.	Ultimate moment (Mu) kN.m EXP.	Mode of failure
Control	110	27.5	CFS buckling
FCH1	164	41	Ferrocement crushing followed by CFS buckling
FCH2	164	41	Ferrocement crushing followed by CFS buckling
FCH3	165	41.25	Ferrocement crushing followed by CFS buckling
FCH4	130	32.5	CFS buckling
FCH5	170	42.5	CFS buckling
FCH6	132	33	CFS buckling
FCH7	185	46.25	CFS buckling
FCH8	136	34	CFS buckling

The nonlinear properties of mortar under tension are based on William and Warnke [16] model as shown in Fig. 14.

Steel Steel is assumed to be isotropic, elastic-perfectly plastic, which behaves identically in tension and compression with stiffness only in the axial direction.

Results and discussion

Tests results

Experimental results in terms of failure load, ultimate moment, and mode of failure of all specimens are tabulated in Table 2. It was found that the presence of a 30-mm ferrocement layer without shear connectors increases the capacity by 18% when compare with the control specimen due to composite action. A linear load-mid span deflection relationship was observed until the formation of the first crack, which is

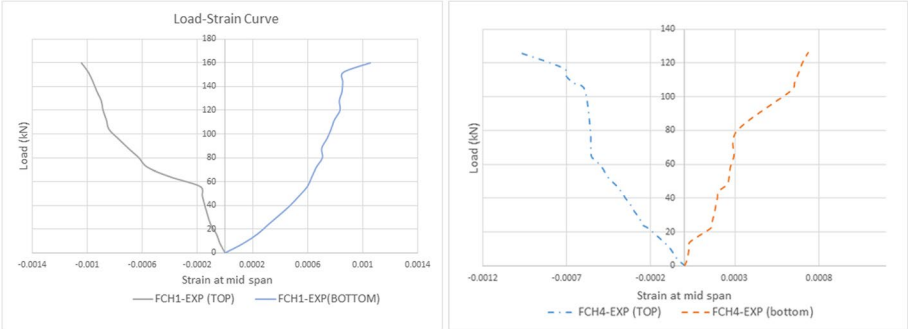

Fig. 15 Load-strain curves at mid-span for FCH1 and FCH4

located under the loading position on the tension side. Figure 15 shows load-strain distributions respectively at mid-span for specimens (FCH1 and FCH4). It can be observed that the presence of shear connectors increases the strain of specimens as they delay buckling. The failure modes observed can be classified into two types: mortar crushing followed by bucking of hollow section or bucking of hollow section only. The failure of specimens (FCH1, FCH2, and FCH3) was governed by ferrocement layer crushing followed by the buckling of cold-formed steel hollow sections simultaneously. However, for specimens (FCH4, FCH5, FCH6, FCH7, and FCH8) the failure was governed by buckling of the cold-formed steel hollow section (CFS) without crushing of ferrocement layer, all specimens' modes of failure are shown in Fig. 16.

No-slip between the ferrocement and hollow section was noticed. All specimens were dismantled after the test in order to investigate shear connectors capacity and hollow steel section buckling shape as shown in Fig. 17. It was noticed that shear connectors experienced little deformation.

Effect of shear connectors

The presence of shear connectors in specimens (FCH1, FCH2, and FCH3) increased the capacity by 26% when compared with (FCH4) (without shear connector). Also, notice that shear connectors increase stiffness and decrease the deflection. Load vs. mid-span deflection curves are plotted in Fig. 18. The presence of shear connectors delays local buckling. However, the spacing of shear connectors has a small effect due to compression failure occurring in mortar.

Effect of mortar thickness

The mortar thickness was studied in specimens (FCH4 and FCH5). It can be seen that the capacity of the section increased by 31% when mortar was increased from 30 mm to 50 mm. However, the deflection decreased when mortar thickness was increased. Figure 19 shows load vs. mid-span deflection curves of the two specimens to show the effect of mortar thickness. As the mortar increased, the stiffness increased due to the increase in the moment of inertia of the section.

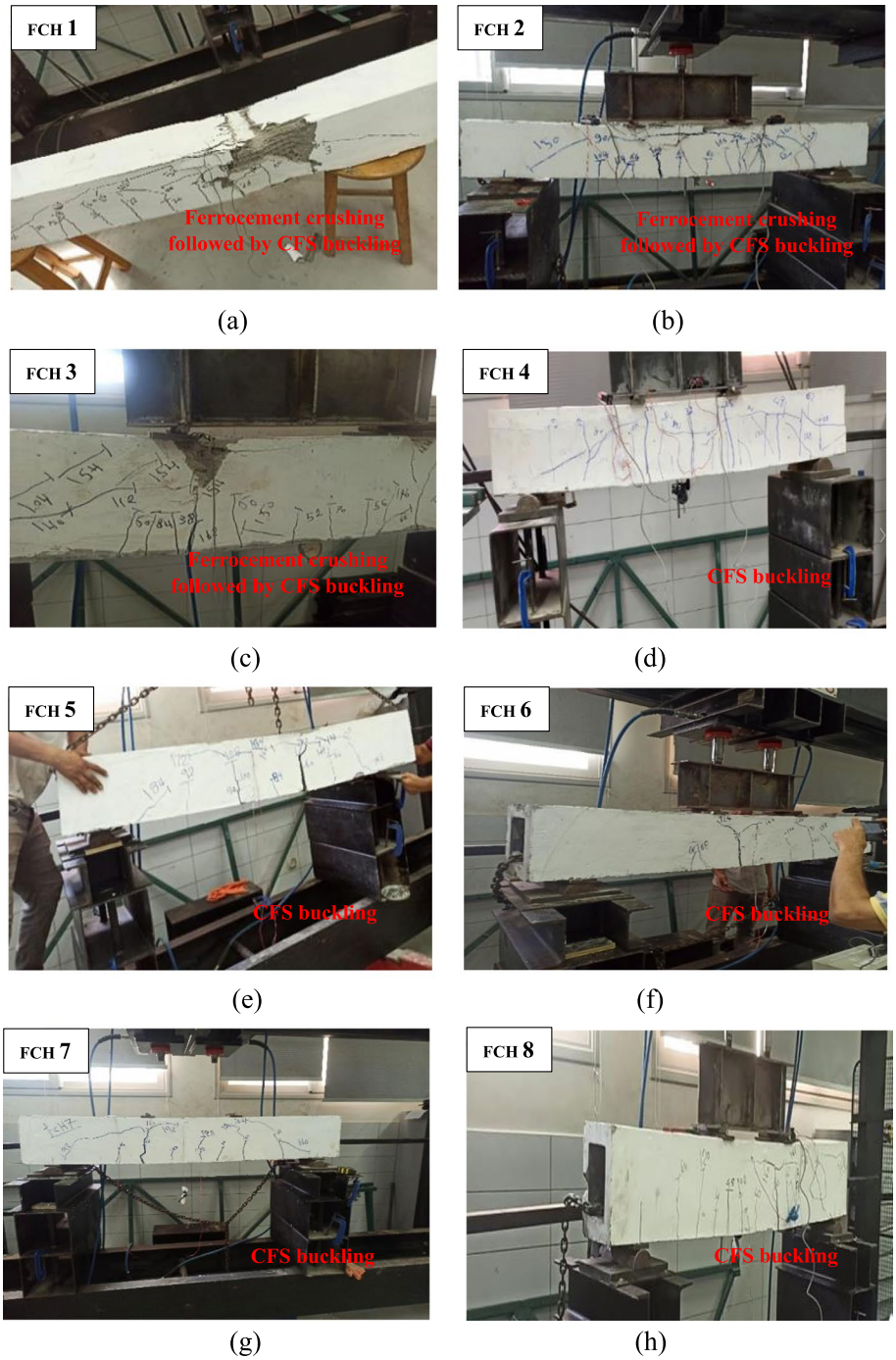

Fig. 16 Specimens failure modes

Effect of hollow steel section thickness on composite section

Steel thicknesses are investigated in specimens (FCH5, FCH6, and FCH7). It can be seen that increasing thickness has a significant effect on the structural behavior of a composite section. Increasing thickness from 2 to 2.5 mm leads to an increase in

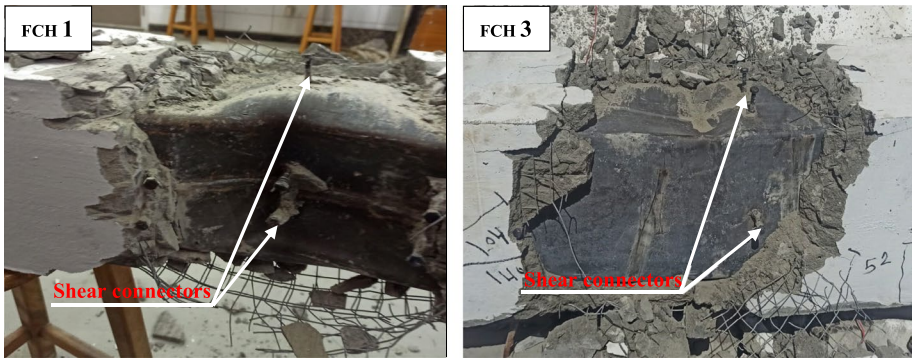

Fig. 17 FCH1 and FCH3 shear connecters after test

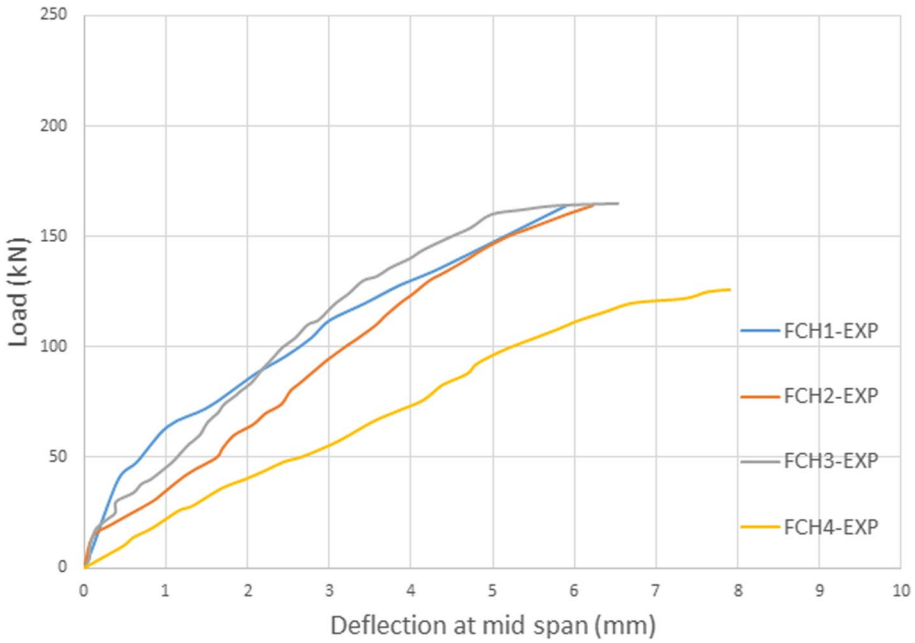

Fig. 18 Load vs. mid-span deflection curves for FCH1, FCH2, FCH3, and FCH4

section capacity of 29%, while increasing thickness from 2 to 3 mm increased the capacity by 40%. Figure 20 shows the load vs. mid-span deflection curves of the three specimens to show the effect of hollow steel section thickness. As CFS increased, the stiffness increased as well and this was due the increase in the moment of inertia of the section.

Effect of increasing surface friction

The increase of surface friction by using diamond plates is being studied. It can be noticed that the change of plate type from ordinary to diamond plate with same thickness has very a small effect on the structural behavior and on the

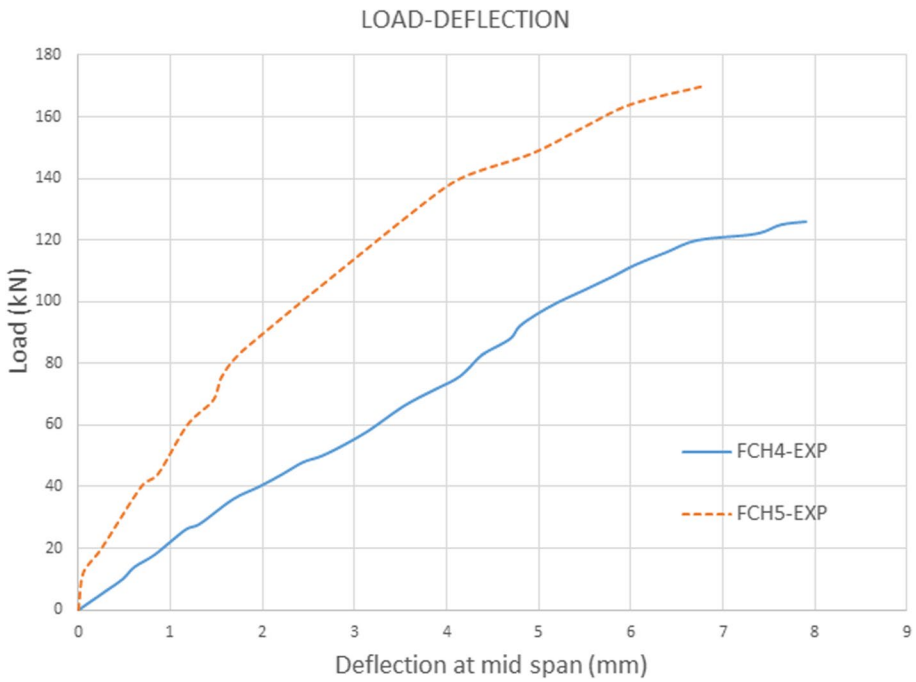

Fig. 19 Load vs. mid-span deflection curves for FCH4 and FCH5

buckling behavior of steel sections which can be neglected. Figure 21 shows the load vs. mid-span deflection curves of the two specimens to show the steel plate type effect.

Comparison of numerical and experimental results

This section compares the results between experimental (EXP) and finite element model (FEM) results for the composite sections. The comparison was made for failure load (Pu), mid-span deflection, and cracks patterns. The obtained results from the experimental data are shown in Fig. 22 with the outputs from finite element models. Figure 23 illustrates the experimental crack pattern and finite element model cracks for FCH1 specimen at various load stages.

The ratio between the results of failure load obtained from both the experimental test (P_{EXP}) and ANSYS (P_{FEM}) was then calculated for all specimens and is tabulated in Table 3. The results show a close agreement between the experimental and finite element results. Therefore, finite element models established in this study can accurately predict the load versus deflection response and failure modes.

Parametric study

Parametric studies were conducted using the finite element method to investigate the effects of hollow steel section thickness, mortar compressive strength (f'c), and the location of the shear connectors on the flexural behavior of the composite beam.

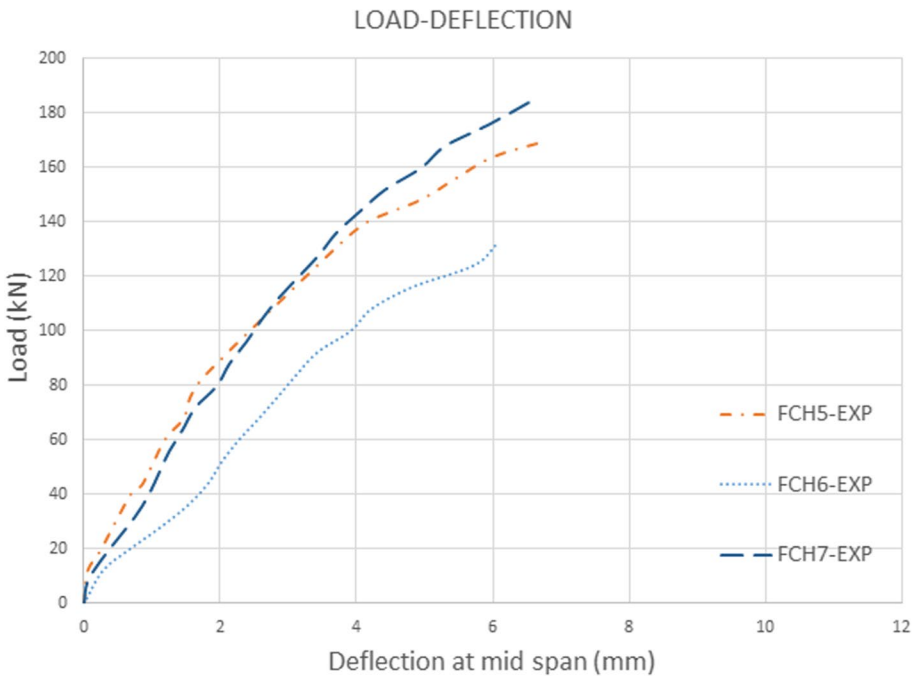

Fig. 20 Load vs. mid-span deflection curves for FCH5, FCH6, and FCH7

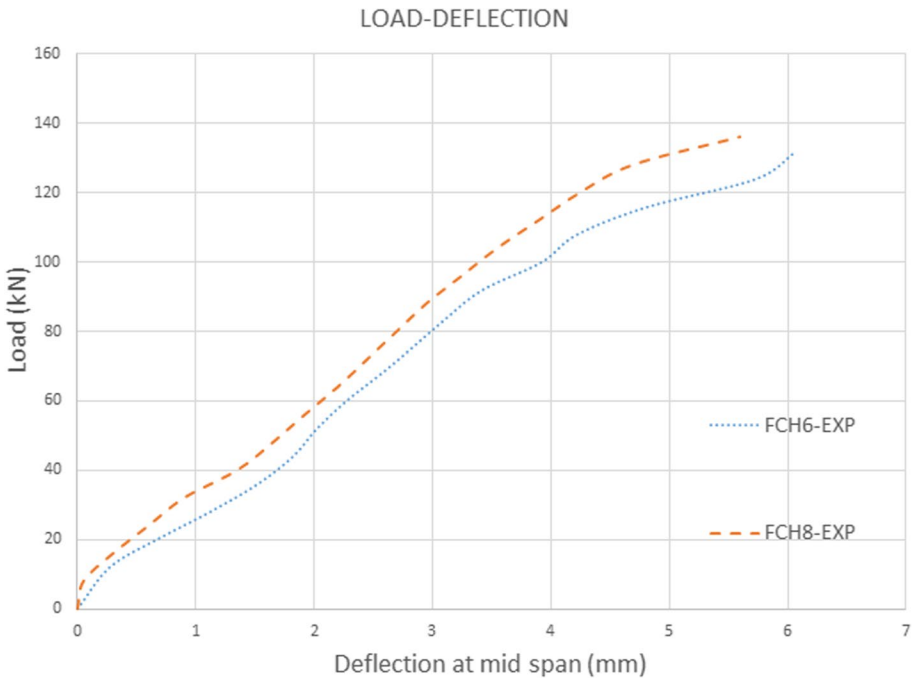

Fig. 21 Load vs. mid-span deflection curves for FCH6 and FCH

Influence of CFS thickness on composite beam capacity

To obtain the effect of cold-formed hollow section thickness (CFS) on composite beam capacity, six FE models with CFS thickness (0.5, 1, 1.5, 2, 2.5, and 3) were analyzed. The

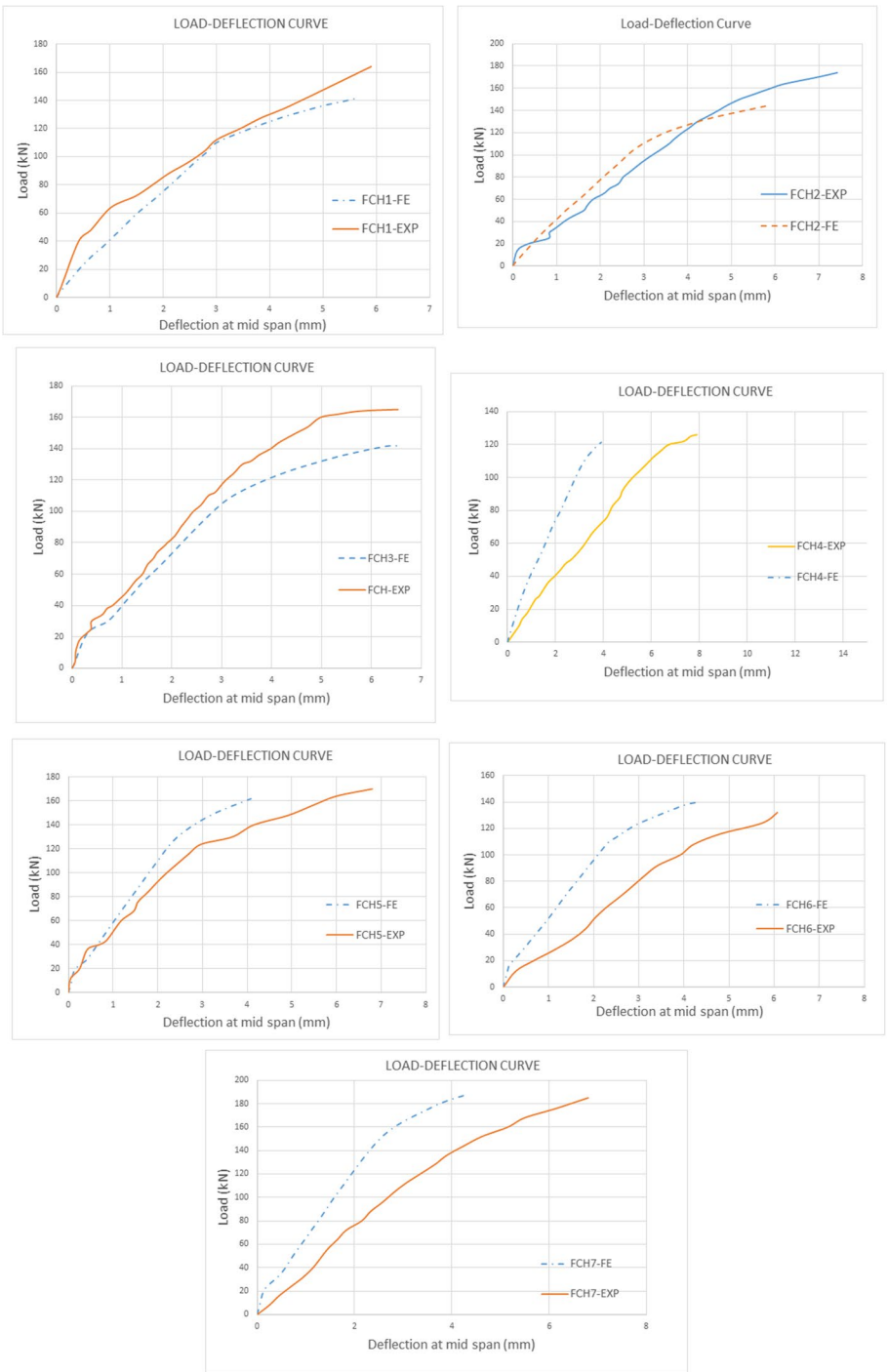

Fig. 22 Experimental and finite element comparison

hollow section dimensions are 180 × 140 mm and the mortar thickness is 50 mm without a shear connector. A failure load-CFS thickness graph is shown in Fig. 24. It can be seen that as thickness increases failure load increases. As CFS decreased, the stiffness

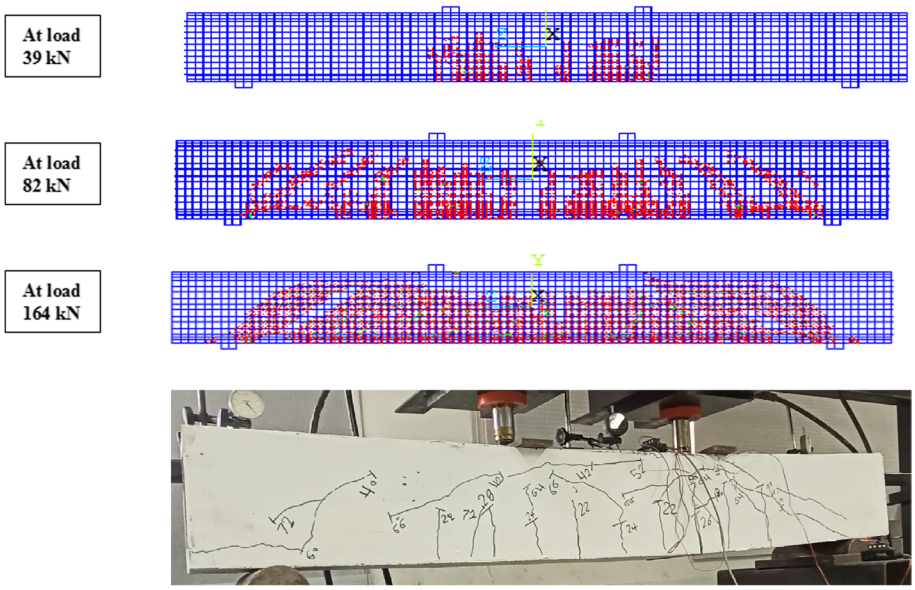

Fig. 23 FCH1 specimen cracks pattern

Table 3 Experimental and finite element results

Specimens ID	Failure load (Pu) kN FEM.	Failure load (Pu) kN EXP.	$(Pu)_{EXP}$ /$(Pu)_{FINITE}$	Max. deflection at mid span (mm) EXP.	Max. deflection at mid span (mm) FEM.
FCH1	142	164	1.15	5.9	5.67
FCH2	142	164	1.15	7	5.77
FCH3	142	165	1.15	6.5	6.5
FCH4	121.5	130	1.07	7.9	4.5
FCH5	161.5	170	1.052	6.8	4.1
FCH6	139.5	132	0.946	6.1	4.25
FCH7	186	185	0.99	6.8	4.25
Mean			1.072		
Standard value deviation			0.077		

decreased as well, and this was due to the decrease in the moment of inertia of the section.

Influence of location of shear connector

To investigate the effect of the location of shear connectors, three models were investigated with a different location for the shear connector as shown in Fig. 25. The spacing of shear connectors for three models is 100 mm. It was found that using two bolts in the upper flange of the hollow section has a very small effect on section capacity when compared with one bolt in middle. The presence of bolts in the web and lower flange of the hollow section also has a very small effect. Load versus mid-span deflection curves are shown in Fig. 26.

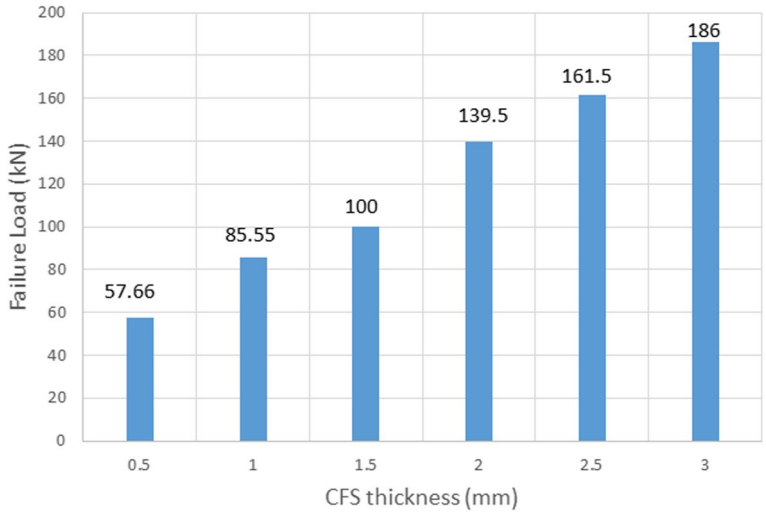

Fig. 24 Failure load–CFS thickness graph

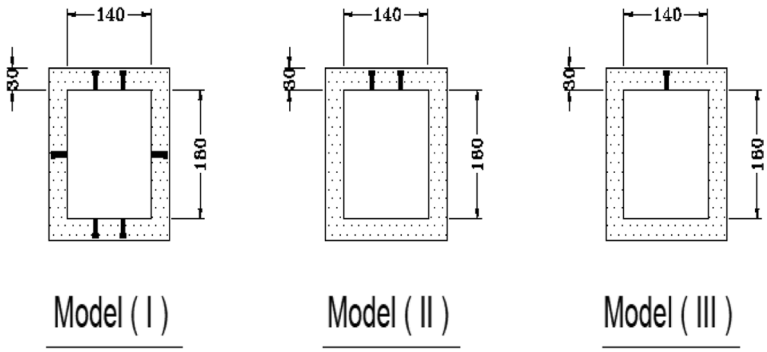

Fig. 25 Shear connector location

Influence of mortar compressive strength (f ′c)

Three finite element models with mortar compressive strengths of 23, 40, and 50 MPa were established to study the effect of concrete compressive strength on composite beam capacity. The section dimensions, CFS thickness, and shear connector spacing are the same as the specimen (FCH1). Load versus mid-span deflection curves are shown in Fig. 27. It can be seen that section capacity increased by 11% when mortar compressive strength increased from 23 to 40 MPa and by about 18 % when compressive strength increased from 23 to 50 MPa. As compressive strength increased, the stiffness increased as well, and this was due to the increase in the moment of inertia of the section. However, the deflection decreased as mortar strength increased.

Conclusions

Based on experimental results and observations of the nine specimens, the following conclusions can be drawn:

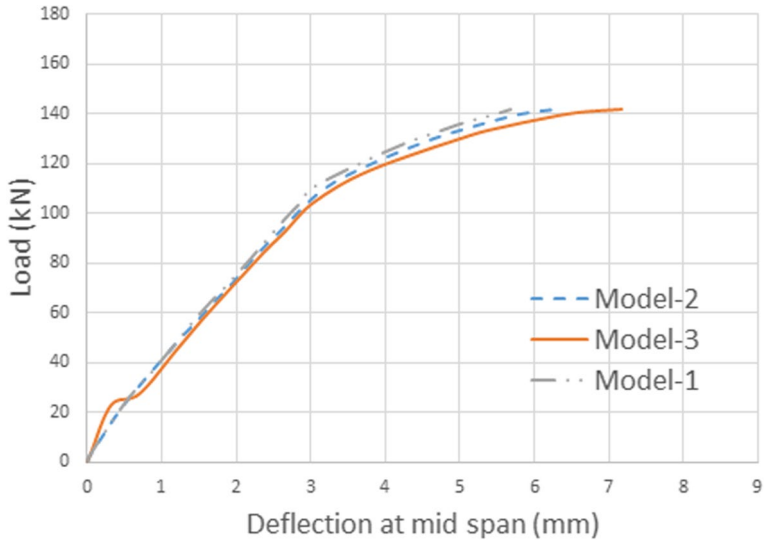

Fig. 26 Failure load–CFS thickness curve

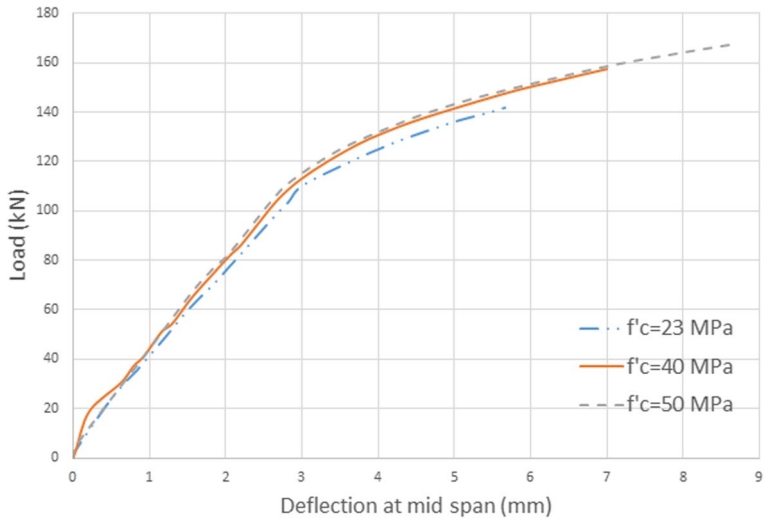

Fig. 27 Load vs. mid-span curves

1. The presence of mortar of a thickness of 3 cm increases section capacity when compared with steel hollow section capacity of dimension (180 × 140 × 2.5 mm) by about 15% due to composite action.
2. Shear connectors increase section capacity by about 30% as they delay local buckling until compression failure of mortar.
3. Increasing mortar thickness leads to an increase in section strength by about 31% due to the increase of the compression zone.
4. The increase in steel thickness section leads to an increase in the capacity ranging from 29 to 40%.
5. The increase in friction between mortar and hollow section caused by using diamond plate has a very small effect on section capacity, which can be neglected.

6. The increase in mortar compressive strength led to an increase in section strength range of 11 to 18%.
7. The effect of the spacing of shear connectors on section capacity is very small, which can be neglected.

Acknowledgements
Not applicable.

Authors' contributions
All authors contributed to the study conception and design. Material preparation, data collection and analysis were performed by Ehab Elkassas, Alaa M Morsy, and Mohamed Marzouck. The first draft of the manuscript was written by Mohamed Marzouck and all authors commented on previous versions of the manuscript. All authors read and approved the final manuscript.

Funding
This research received no specific grant from any funding agency in the public, commercial, or not-for-profit sectors.

Availability of data and materials
Some or all data, models, or code that support the findings of this study are available from the corresponding author upon reasonable request.

Declarations

Competing interests
The authors declare that they have no competing interests.

Received: 20 April 2022 Accepted: 16 July 2022
Published online: 30 September 2022

References

1. ANSI/AISC 360-10 (2016) Specification for structural steel buildings. American Institute of Steel Construction (AISC), Chicago
2. BS5950-1 (2000) Structural use of steelwork in building: code of practice for design. British Standards Institution, London
3. AS/NZS4600 (2005) Cold-formed steel structure. Standards Australia/Standards New Zealand, Sydney
4. EN 1993-1-1 (2005) Design of steel structures–Part 1.1: general rules and rules for buildings. European Committee for Standardization, Brussels
5. Jouaux R (2004) The plastic behavior of cold-formed SHS (square hollow sections) under bending and compression, Diploma Thesis, Department of Civil Engineering
6. ACI Committee 549-1R-88, Guide for design construction and repair of ferrocement, ACI 549-1R-88 and 1R-93 manual of concrete practice, Detroit, 1993.
7. Naaman AE (2000) Ferrocement and Laminated Cementitious Composites. Techno Press 3000, Ann Arbor
8. Alhajri TM, Tahir MM, Azimi M, Lawan MM, Alenezi KK, Ragaee MB (2016) Behavior of pre-cast U-Shaped Composite Beam integrating cold-formed steel with ferro-cement slab. Thin-Walled Struct 102:18–29
9. Hsu CT, Punurai S, Punurai W, Majdi Y (2014) New composite beams having cold-formed steel joists and concrete slab. Eng Struct 71:187–200
10. El-Sayed KM, Debaiky AS, Nader NK, El-Shenawy IM (2019) Improving buckling resistance of hollow structural steel columns strengthened with polymer-mortar. Thin-Walled Struct 137:515–526
11. ESS No. 373 (1991) Portland cement, ordinary, and rapid hardening. Egyptian Standard Specifications Ministry of Industry, Cairo
12. ECCS 203 (2004) Egyptian code of practice for design and construction of reinforced concrete structures, 2nd edn, p 209
13. Azimi M, Bin Adnan A, Tahir M, Sam AR, Razak SKA (2015) Seismic performance of ductility classes medium RC beam-column connections with continuous rectangular spiral transverse reinforcements. Lat Am J Solids Struct 12(4):787–807
14. Lorenc W, Kubica E (2006) Behavior of composite beams pre-stressed with external tendons. J Constr Steel Res 62:1353–1366
15. Desayi P, Krishnan S (1964) Equation for the stress-strain curve of concrete. J Am Concr Inst 61:345–350
16. William KJ, Warnke EP (1975) Constitutive model for the triaxial behavior of concrete. In: International Association for Bridge and Structural Engineering. ISMES, Bergamo

Publisher's Note